FINITE ELEMENT ANALYSIS OF FINITE DEFORMATION PROBLEMS FOR BIO-POLYMER MATERIALS

Pin-Jun Chen[1], Bo-Sen Chuang[1] and Chien-Kai Wang[2]

[1] *Civil Engineering, Tamkang University, Taiwan*

[2] *Faculty of Civil Engineering, Tamkang University, Taiwan*

ABSTRACT

For shape maintenance and migration of living organisms, bio-polymer materials play important roles for the redistribution of internal forces in the biological structures. A substantial amount of observations have been made over the past decades to show how the structures composed of bio-polymers deform and identify what the characteristics of the network materials are. For example, it has been revealed both experimentally and computationally that as macroscopic loading goes, the bio-polymer materials of the network type experience alterations from entropy-directed shape changes to structural deformations, such as filament bending and stretching. In addition, the transition point happens as the levels of macroscopic stress reach around 1% of the bulk modulus of the materials (Lin *et al.* 2014). Hence, here finite element formulations are developed to solve the large deformation problems for the bio-polymer materials in solutions by introducing fluid-solid interaction forces across the immersed boundaries of the materials. We anticipate that this technique will open doors for understanding more physiological states of biological specimens under environmental loading.

Keywords: Finite element method, fluid-solid interaction, soft materials, nonlinear elasticity.

1. INTRODUCTION

For recent decades, a great amount of investigation efforts have been put into the fluid-solid interaction naturally occurring in wide-range of engineering problems and physical phenomena. To realize the fluid-structure interaction complexity, mechanics of fluid-solid boundaries has to be accomplished thoroughly in different models. Through the models of computational mechanics, the research achievements facilitate challenging engineering applications, for example, geo-mechanical engineering, soil-structure interaction, microelectromechanical systems, and microfluidic devices. Here, the goal of this research is to implement the modern finite element analysis for solving fluid-solid interaction problems. The formulations of mechanics which embrace conservation equations, kinematics descriptions and computing algorithms especially developed for elaborating fluid-solid interaction models are also the main theme of this paper.

2. FORMULATIONS OF FINITE ELEMENT METHOD FOR FLUID-SOLID INTERACTION

We may consider the finite element method for solving fluid-solid interaction problems under the following three main subjects: the boundary force mapping from solids to fluids, the boundary value problem in solid mechanics, and the model problem of viscous incompressible fluids in fluid dynamics. The detailed description of the finite element method dealing with the interaction between fluids and nonlinear elastic solids with large deformations will be given in this section.

2.1. Boundary force mapping from solids to fluids

The framework named as the immersed boundary (IB) method for solving the fluid-solid interaction problems was initially developed by Peskin to investigate blood fluids through a heart valve structure (Peskin 1972). In this framework, various fluid-structure interaction problems can be elucidated through the boundary force mapping from the solid to the fluid. The immersed boundary between the solid and fluid is considered as a zone directly blending the fluid-solid interactions into forces acting the neighboring fluid and solid (Peskin 2002). The concept of the fluid-solid finite element formulations in this paper is an adaptation of Peskin's IB method. Having got the special framework out of Peskin's work, we may turn to our central idea of dealing fluid-solid interactions in finite element formulations that the interaction of fluids with deformable solids is through the forces exerted onto the fluids by the adjacent solids across the immersed boundary. In continuum, the interaction forces subjected to elastic solids and incompressible Newtonian fluids act as externally applied body forces along the boundary appearing in the linear momentum balance equations of the solids with assured traction boundary conditions and the Navier-Stoke equations of the fluids respectively:

$$\sigma_{ij,j} + \rho^s b_i = \rho^s \ddot{u}_i \quad \text{subjected to} \quad n_j \sigma_{ij} = f_i^s \quad \text{on the immersed boundary} \quad \partial\Omega^s, \tag{1}$$

$$\rho^f \left(\frac{\partial v_i}{\partial t} + v_j v_{i,j} \right) + p_{,i} = \mu v_{i,jj} + f_i^f \quad \text{and} \quad v_{i,i} = 0, \tag{2}$$

where $\boldsymbol{\sigma}$ is the Cauchy stress field, $\mathbf{b}$ is the body force distribution, $\mathbf{u}$ is the displacement field in the solid domain Ω^s, $\mathbf{f}^s$ is the traction distribution on $\partial\Omega^s$, $\mathbf{v}$ is the velocity field, $\mathbf{p}$ is the pressure distribution, $\mathbf{f}^f$ is the external force at time t in the fluid domain Ω^f, and ρ^s and ρ^f are the mass density of the solids and fluids correspondingly. In this paper, the superscript s represents quantities for solids, while f for fluids. Here, we assume that the externally body forces are applied relatively slowly compared to environmental chemical loadings on the solid surfaces. Hence, in certain circumstances, the solid is in quasistatic equilibrium, and its inertial effects can be reasonably ignored. Furthermore, the equilibrium equations in terms of stresses can be replaced with an integral expression which is namely weak form by the principle of virtual work

(PVW) for finite element analysis in solid mechanics. The integral version of the equilibrium equations is thus derived as

$$\int_{\Omega^s} \sigma_{ij} \delta u_{i,j} dV = \int_{\Omega^s} \rho^s b_i \delta u_i dV + \int_{\partial\Omega^s} f_i^s \delta u_i dS . \tag{3}$$

The PVW states that if the stress field satisfies the weak form for all kinematically admissible virtual displacement fields δu_i, it will automatically satisfy the equilibrium equation and the traction boundary conditions presented in Equation (1). In this study, we are proposing that fluid-solid interaction forces acting on the neighboring fluid and solid particles are naturally action and reaction to each other satisfying Newton's third law. To advance the finite element formulation for fluid-solid interaction problems, we apply the algorithm developed by Peskin for mapping boundary forces from a solid surface onto its adjacent fluid particles (Peskin 2002)

$$f_i^f \left(\mathbf{x}^f, t \right) = -\int_{\partial\Omega^s} f_i^s \left(s, t \right) \delta \left(\mathbf{x}^f - \mathbf{x}^s \left(s, t \right) \right) dS , \tag{4}$$

where $\mathbf{x}^s \left(s, t \right)$ is a parametric immersed boundary configuration of the solid domain, $f_i^f \left(\mathbf{x}^f, t \right)$ is the external force at location $\mathbf{x}^f$ along the boundary and time t in the fluid domain, and $\delta(\mathbf{x}^f)$ is a Dirac delta function.

2.2. Boundary value problem in solid mechanics

To understand mechanical responses of biological specimens under environmental loading related to possible physiological states, we consider a hyperelastic material model with the Neo-Hookean material description including nonlinear material behaviors and large shape changes for an isotropic solid. In continuum mechanics, the deformation measurements commonly used in large strain elasticity are the deformation gradient F_{ij}, the Jacobian of the deformation gradient field J, and the Left Cauchy-Green deformation tensor B_{ij}. In addition, the constitutive law of stress-strain relation for an isotropic hyperelastic material is defined by an energy function relating the strain energy density of the material to its deformation gradient. The strain energy density to the deformation gradient of a generalized Neo-Hookean solid is

$$\overline{U} = \frac{\mu_1}{2} \left(\overline{I}_1 - 3 \right) + \frac{\kappa_1}{2} \left(J - 1 \right)^2 , \tag{5}$$

where μ_1 and κ_1 are the shear and bulk modulus of the solid respectively, and $\overline{I}_1$ is $B_{kk} / J^{2/3}$.

For such finite strain problems, it is usually more convenient to evaluate the integrals appearing in the weak form of equilibrium equations over reference configurations, whereas the deformed configuration is unknown:

$$\int_{\Omega_0^s} \tau_{ij} F_{mj}^{-1} \frac{\partial \delta u_i}{\partial X_m^s} dV_0 = \int_{\Omega_0^s} \rho_0^s b_i \delta u_i dV_0 + \int_{\partial \Omega_0^s} f_i^s \delta u_i \eta dS_0 \,, \tag{6}$$

where τ_{ij} is Kirchhoff stress tensor, and η is the inverse surface Jacobian. Then, we apply the typical finite element approach for solving the nodal displacement on a set of meshes in an undeformed solid by introducing the usual finite element interpolation written as

$$u_i\left(\mathbf{X}^s\right) = \sum_{a=1}^{n} N^a\left(\mathbf{X}^s\right) u_i^a \,, \tag{7}$$

where $N^a\left(\mathbf{X}^s\right)$ is the shape function, u_i^a is the nodal displacement, and n is the number of nodes for an element in the meshes. Subsequently, the virtual work equation becomes

$$\int_{\Omega_0^s} \tau_{ij} \left[F_{pq}\left(u_k^b\right) \right] \frac{\partial N^a}{\partial X_m^s} F_{mj}^{-1} dV_0 = \int_{\Omega_0^s} \rho_0^s b_i N^a dV_0 + \int_{\partial \Omega_0^s} f_i^s N^a \eta dS_0 \,. \tag{8}$$

Now this is the system of nonlinear equations for the unknown nodal displacement u_k^b. One may notice that the nonlinear behaviors of the solid are resulted from both material properties and geometry configurations. To solve the nonlinear virtual work equation, we apply the Newton-Raphson iteration algorithm by guessing the solution for nodal displacement as w_k^b and perturb it as $w_k^b + dw_k^b$. The equilibrium equation thus yields a system of linear equations by ignoring high order terms for solving dw_k^b in iteration progress as

$$K_{aibk} dw_k^b + R_i^a - F_i^a = 0 \,, \tag{9}$$

where

$$K_{aibk} = \int_{\Omega_0^s} \frac{\partial \tau_{ij}}{\partial F_{kq}} \frac{\partial N^b}{\partial X_q^s} \frac{\partial N^a}{\partial X_m^s} F_{mj}^{-1} dV_0 + \int_{\Omega_0^s} \tau_{ij} \frac{\partial N^a}{\partial X_m^s} F_{mk}^{-1} \frac{\partial N^b}{\partial X_q^s} F_{qj}^{-1} dV_0 - \int_{\partial \Omega_0^s} f_i^s N^a \frac{\partial \eta}{\partial u_k^b} dS_0 \,, \tag{10}$$

$$R_i^a = \int_{\Omega_0^s} \tau_{ij} \frac{\partial N^a}{\partial X_m^s} F_{mj}^{-1} dV_0 \,, \text{ and} \tag{11}$$

$$F_i^a = \int_{\Omega_0^s} \rho_0^s b_i N^a dV_0 + \int_{\partial \Omega_0^s} f_i^s N^a \eta dS_0 \,. \tag{12}$$

2.3. Model problem of viscous incompressible fluids in fluid dynamics

In many fluid-structure interaction problems, the fluid density is reasonably set as a constant in certain ambient condition. For this kind of problems, the systems of equations are suggested to be solved by the discrete Fourier transform, implemented by the Fast Fourier Transform algorithm. To facilitate the implementation, the models for solving the problems are formulated on periodic domains (Peskin and McQueen 1996). The Navier-Stoke equations of the incompressible Newtonian fluids shown in equation (2) may be discretized by introducing the central difference operator $D_{h,i}^0$, the skew-symmetric difference operator $S_h(\mathbf{v})$ (Peskin 2002), and the tight Laplacian operator L_h as follows:

$$\rho^f\left(\frac{\partial v_i}{\partial t}+S_h(\mathbf{v})v_i\right)+D_{h,i}^0 p=\mu L_h v_i+f_i^f \quad \text{and} \quad D_{h,i}^0 v_i=0, \tag{13}$$

where

$$D_{h,i}^0 p=\frac{p\left(\mathbf{x}^f+h\mathbf{e}_i\right)-p\left(\mathbf{x}^f-h\mathbf{e}_i\right)}{2h}, \tag{14}$$

$$S_h(\mathbf{v})v_i=\frac{1}{2}v_j D_{h,j}^0 v_i+\frac{1}{2}D_{h,j}^0\left(v_i v_j\right), \text{ and} \tag{15}$$

$$L_h v_i=\sum_{j=1}^3 \frac{v_i\left(\mathbf{x}^f+h\mathbf{e}_j\right)+v_i\left(\mathbf{x}^f-h\mathbf{e}_j\right)-2v_i\left(\mathbf{x}^f\right)}{h^2}. \tag{16}$$

To further improve numerical stability, a temporal discretization scheme with two substeps based on the second-order accurate Runge-Kutta method proposed by Lai and Peskin (Lai and Peskin 2000) is used for the above system of ordinary differential equations. The preliminary substep, from level n to $n+1/2$, proceeds as follows:

$$\frac{x_i^{s,n+1/2}(s)-x_i^{s,n}(s)}{\Delta t/2}=\sum_{\mathbf{x}^f}v_i^n\left(\mathbf{x}^f\right)\delta_h\left(\mathbf{x}^f-\mathbf{x}^{s,n}(s)\right)h^2, \tag{17}$$

$$f_i^{f,n+1/2}\left(\mathbf{x}^f\right)=-\sum_{\mathbf{x}^s}f_i^{s,n+1/2}(s)\delta_h\left(\mathbf{x}^f-\mathbf{x}^{s,n+1/2}(s)\right)\Delta s, \tag{18}$$

$$\rho\left(\frac{v_i^{n+1/2}-v_i^n}{\Delta t/2}+S_h\left(\mathbf{v}^n\right)v_i^n\right)+D_{h,i}^0 \tilde{p}^{n+1/2}=\mu L_h v_i^{n+1/2}+f_i^{f,n+1/2}, \text{ and } D_{h,i}^0 v_i^{n+1/2}=0 \tag{19}$$

Note that Equation (19) forms a system of equations with the unknowns $v_i^{n+1/2}$ and $\tilde{p}^{n+1/2}$ for $\mathbf{x}^f$.

Similarly, the final substep, from level n to $n+1$, proceeds as follows:

$$\frac{x_i^{s,n+1}(s) - x_i^{s,n}(s)}{\Delta t} = \sum_{\mathbf{x}^f} v_i^{n+1/2}(\mathbf{x}^f) \delta_h(\mathbf{x}^f - \mathbf{x}^{s,n+1/2}(s)) h^2 , \qquad (20)$$

$$\rho\left(\frac{v_i^{n+1} - v_i^n}{\Delta t} + S_h(\mathbf{v}^{n+1/2}) v_i^{n+1/2}\right) + D_{h,i}^0 p^{n+1/2} = \mu L_h\left(\frac{v_i^n + v_i^{n+1}}{2}\right) + f_i^{f,n+1/2} , \text{ and } D_{h,i}^0 v_i^{n+1} = 0 \qquad (21)$$

Again, note that Equation (21) forms a system of equations with the unknowns v_i^{n+1} and $p^{n+1/2}$ for $\mathbf{x}^f$.

3. NUMERICAL EXAMPLE

A close study on nanoindentation of hydrated collagen fibrils was made by Grant *et al.*, and it revealed that the elastic modulus E of individual collagen fibrils can be varied over a range of 1.938-4.762 MPa in variation of sodium chloride solutions in water of 0-1 M concentration at pH 7 (Grant *et al.* 2009). In this section, we will examine oscillations in the transverse direction of the cross section of an initially deformed collagen fibril in solutions with different NaCl concentrations. Consider the undeformed and initially deformed configurations of the cross section of the collage fibril parameterized respectively by

$$\mathbf{X}^s(s,0) = \left[1/2 + r\cos(s), 1/2 + r\sin(s), 0\right]^T , \text{ and} \qquad (22)$$

$$\mathbf{x}^s(s,0) = \mathbf{X}^s(s,0) + \lambda\left[0, r\sin(s), 0\right]^T , \text{ where } \lambda = \begin{cases} -1/10 & ; \left|X_2^s - 1/2\right| / r \geq 1/\sqrt{2} \\ 0 & ; \text{ otherwise} \end{cases} . \qquad (23)$$

In general, the Poisson's ratio of collagen fibrils, which reflect the effect of network heterogeneity under macroscopic deformation fields and the realignment of the fibers, was reported 0.27 for the transverse direction of the fiber-aligned orientation in soft biological tissues by Stylianopoulos (Stylianopoulos 2008). Besides, the density and viscosity of sodium chloride solutions in water were systematically measured at 298.15 K by Zhang and Han (Zhang and Han 1996). Accordingly, we adopt these measured material properties of collagen fibrils and sodium chloride solutions in water of different concentrations which are listed in Table 1. This example is designed to solve the oscillation in transverse direction of the cross section of the initially deformed collagen fibril in solutions of different NaCl concentrations. The fluid domain has a size of 1×1 cm, and the geometry property of $r = 0.2$ cm is set for the solid domain. Figure 1 shows the stress fields of the cross section of the collagen and fluid velocity contours in the NaCl solution in water of 0.50 M at different time steps. One may also observe the progress of collagen fibril oscillation through these deformed configurations.

Using the parameters described above, we can examine further the strain energy evolution of the collagen in sodium chloride solutions during its oscillation progress through finite element analysis.

Table 1: Material properties of collagen fibrils in solutions of different NaCl concentrations

Material property\Case	I	II	III	IV	V
Fluid					
Molar concentration C (M)	0.00	0.25	0.50	0.75	1.00
Density ρ (g/cm^3)	0.9969	1.0071	1.0166	1.0261	1.0349
Viscosity μ (mPa-s)	0.8911	0.9111	0.9309	0.9512	0.9722
Solid					
Elastic modulus E (MPa)	2.138	1.938	2.486	3.005	4.762

Figure 2 presents the comparison with the evolution of the ratio of the total strain energy to that at $t = 0$ of the collagen material in NaCl solutions with various concentrations. Besides, the inset presents the deformed configurations of the collagen material and velocity contours in the saline solutions with case I and V at time of 0.28 milliseconds. The results clearly illustrate that the collagen fibril becomes laxer along the transverse directions of its cross section while staying in the solution with lower concentrations of NaCl.
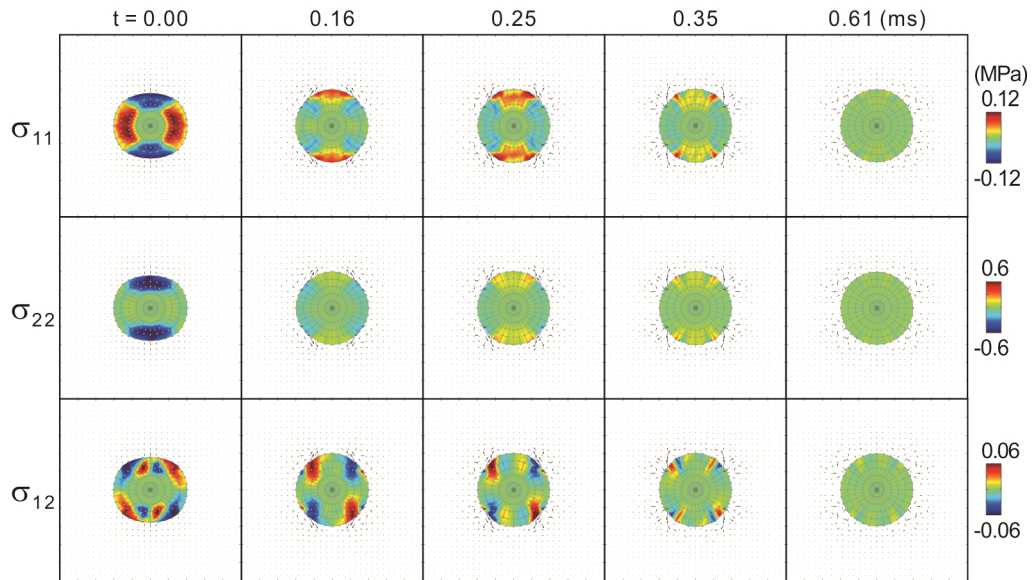
Figure 1: The stress fields of the cross section of a collagen fibril in the sodium chloride solution in water of 0.50 M concentration at different time steps.

4. CONCLUSIONS

In this study, we proposed the finite element algorithm for considering the fluid-solid interaction forces acting on the neighboring fluid and solid particles as naturally action and reaction to each other satisfying Newton's third law. As the computational results presented in this paper, this algorithm provides a unique way of analyzing mechanics problems of bio-polymer materials subjected environmental loading in fluids.
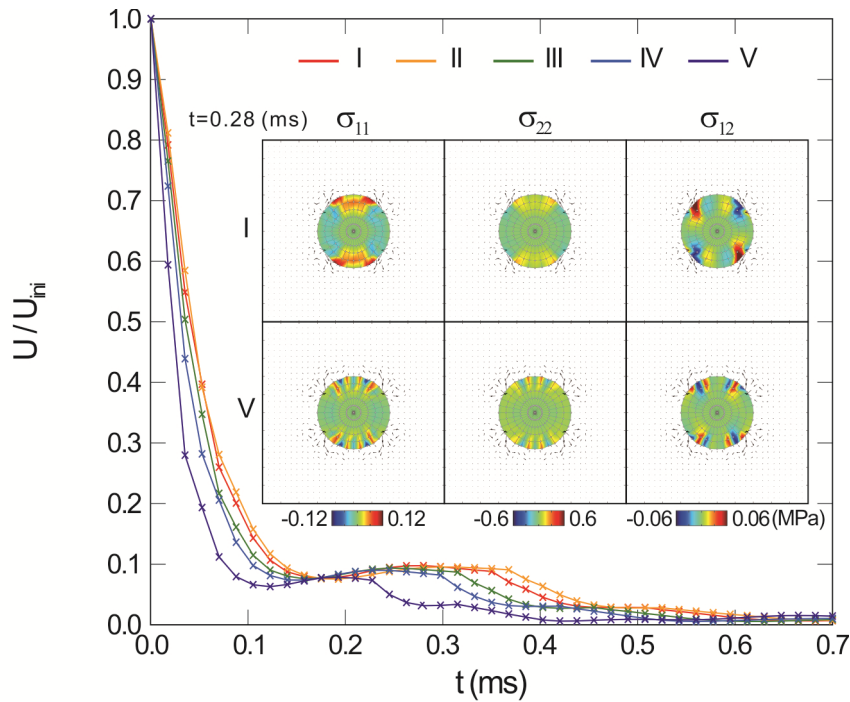
Figure 2: Comparison with the evolution of the ratio of the total strain energy to that at t = 0 of the collagen fibril in NaCl solutions of various concentrations. Inset: Stress fields of the cross section at t = 0.28 (ms).

5. ACKNOWLEDGMENTS

6. REFERENCES

Grant, C. A., Brockwell, D. J., Radford, S. E., and Thomson, N. H. (2009). "Tuning the elastic modulus of hydrated collagen fibrils." Biophys. J., 97, 2985-2992.

Lai, M.-C. and Peskin, C. S. (2000). "An immersed boundary method with formal second-order accuracy and reduced numerical viscosity." J. Comp. Phys., 160(2), 705-719.

Lin, Y., Wei, X., Qian, J, Sze, K.Y. and Shenoy, V.B. (2014). "A combined finite element-Langevin dynamics (FEM-LD) approach for analyzing the mechanical response of bio-polymer networks." J. Mech. Phys. Solids, 62, 2-18.

Peskin, C. S. (1972). "Flow patterns around heart valves: A numerical method." J. Comp. Phys., 10(2), 252-271.

Peskin, C. S. (2002). "The immersed boundary method." Acta Numer., 11, 479-517.

Peskin, C. S. and McQueen, D. M. (1996). "In case studies in mathematical modeling: Ecology, physiology, and cell biology." Prentice-Hall, Eaglewood Cliffs, New Jersey, 313-342.

Stylianopoulos, T. (2008). Multiscale mechanical modeling of soft biological tissues, Ph.D. Thesis, University of Minnesota.

Zhang, H.-L. and Han, S.-J. (1996). "Viscosity and density of water + sodium chloride + potassium chloride solutions at 298.15 K." J. Chem. Eng. Data, 41, 516-520.